Front. Optoelectron. China 2008, 1(3–4): 329–335
DOI 10.1007/s12200-008-0081-6

RESEARCH ARTICLE

Theoretical and experimental research on Er-doped and Yb-Er co-doped Al_2O_3 waveguide amplifiers

Shufeng LI (✉)[1], Chengren LI[1,2], Changlie SONG[1]

1 Physics Department, Dalian University of Technology, Dalian 116023, China
2 Physics Department, Liaoning Normal University, Dalian 116029, China

Abstract The rate equations of Er-doped and Yb-Er co-doped systems pumped at 0.98 μm are presented, with consideration for the upconversion mechanisms such as cooperative upconversion, cross relaxation, and excited state absorption. A multi-theoretical model is founded to analyze the gain characteristics of Er-doped and Yb-Er co-doped Al_2O_3 waveguide amplifiers by using rate equations, a two-dimension waveguide finite element model and propagation equations with forward and backward amplified spontaneous emission. The dependence of the gain on amplifier length, pump power and doping concentration is obtained. The optimum design curve is given for designing waveguide amplifiers. The new theory is used to analyze the gain performance of a practical Yb-Er co-doped Al_2O_3 waveguide amplifier, and the analyzed results are in accordance with the experimental data.

Keywords integrated optics, Er-doped Al_2O_3 waveguide amplifier (EDAWA), Yb-Er co-doped Al_2O_3 waveguide amplifier (YEDAWA), multi-theoretical model, net gain

1 Introduction

The 1.53 μm Er-doped and Yb-Er co-doped waveguide amplifiers (EDWA, YEDWA) have attracted great attention in the research on active devices in all-optical communication because of their potential for having small sizes [1–3], low cost, stable and reliable performance and the possibility of integration with other components such as pump lasers, switches, filters, couplers and wavelength division multiplexers.

Currently, EDWAs with a variety of host material for Er have been studied, such as Si, SiO_2, phosphate glass, sodium calcium silicate glass, $LiNbO_3$ and Al_2O_3 [4,5]. Especially, Er-doped Al_2O_3 waveguide amplifier (EDAWA) and Yb-Er co-doped Al_2O_3 waveguide amplifier (YEDAWA) have attracted more attention [6]. First, the high confinement, low-loss transmission and small bend radius can be realized because of the large refractive index changes between Al_2O_3 and the buffer layer (SiO_2), and the cover layer [4]. Second, due to the similar crystal structures between Al_2O_3, Er_2O_3 and Yb_2O_3, high gain can be achieved in a small size with high concentration incorporation of Er and Yb. The absorption spectra of Er^{3+} and emission spectra of Yb^{3+} have greater overlap [7], the absorption cross-section Yb^{3+} at 0.98 μm is about an order of magnitude larger than that of Er^{3+}, and the pumping efficiency by co-doping Yb can be greatly improved through energy transmission between Yb^{3+} and Er^{3+}.

In 1996, Hoven et al. studied a 4-cm Er-doped Al_2O_3 waveguide amplifier integrated onto a silicon chip with an area of 15 mm^2 [8]. Recently, the research group developed an Er-Yb co-doped Al_2O_3 waveguide in the laboratory [9].

Chryssou et al. theoretically studied the gain of an Er-Yb co-doped Al_2O_3 channel waveguide amplifier with a 2 μm × 2 μm cross-section [10]. However, for this waveguide structure, a signal light propagates with a non-single mode. In theoretical calculations, the result of whether the absorption and emission cross-sections of Er or Yb in an Al_2O_3 host material replaced by that in glass or other materials [10,11] are limited and imprecise due to the lack of relevant experimental data on Er-doped Al_2O_3 film materials or amplified spontaneous emission and the upconversion mechanism are neglected [12].

In order to analyze the performance of the amplifier gain influenced by more factors so as to achieve a reasonable design optimization in technology, a multi-theoretical model is founded. The model consists of three interrelated parts: a) the components of the guiding mode and field distribution at signal and pumping wavelengths determined by waveguide geometry structure, physical

Translated and revised from *Acta Optica Sinica*, 2007, 27(5): 928–934 [译自: 光学学报]

E-mail: sf.lee@163.com

parameters and coupled conditions between the fiber and waveguide by the finite element method (FEM); b) the rate equation with an eight-level system for Er^{3+} and Yb^{3+} to calculate the particle distribution of each level, considering the active particles' (Er^{3+} and Yb^{3+}) linear and nonlinear mechanisms such as absorption, emission, upconversion and cross relaxation; c) the propagation equation to show the evolution of the signal light, pumping light and the forward or backward spontaneous emission along the waveguide. The optimum design curve of amplifier gain is obtained, which can be used to design EDAWA and YEDAWA including the doping concentration, etching size, waveguide length and pump power.

2 Multi-theoretical model

2.1 Guiding modes and field distributions

Waveguide design should assure single-mode operation at signal wavelength to enhance coupling efficiency between fiber and waveguide and to avoid mode dispersion in the amplification process. However, pump light, which can remain in a multi-mode state, is not like that. The mode field and normalized intensity distribution are calculated by FEM for a different rib height waveguide with a 1-μm thick active layer and a 3-μm etching width. By comparison, under the conditions of the single-mode, a high confinement of mode field and far away from the cut-off mode, the 0.8-μm rib height is more appropriate [13].

The parameters of the rib waveguide are shown in Fig. 1. Two fundamental modes $\left(E_{11}^x \text{ and } E_{11}^y\right)$ can propagate at 1.53 μm wavelength, whereas the other six modes $\left(E_{11}^x, E_{11}^y, E_{21}^x, E_{21}^y, E_{31}^x, E_{31}^y\right)$ do so at 0.98 μm wavelength. The single-mode for 1.53 μm can be realized through polarized excitation. It is assumed that the signal and pumped light are directly coupled into the waveguide from the fiber. The input total electromagnetic field can be expressed in an expanded eigenmode field. The mode excitation fraction is $\alpha_i = c_i c_i^* \Big/ \sum_{i=1}^{N} c_i c_i^*$, where c_i is the expanded coefficient of the ith guiding mode, c_i has a relation to the field distribution of the fiber output and position offset due to the misalignment of the fiber and waveguide in coupling [14]; N is the number of guiding modes excited by the signal or pumped light. In the cross-section of the waveguide, the total normalized intensity distributions of signal and pump are as follows, respectively:

$$\psi_s(x,y) = \sum_{i=1}^{N_s} \alpha_{si}\psi_{si},$$

$$\psi_p(x,y) = \sum_{i=1}^{N_p} \alpha_{pi}\psi_{pi}.$$

In addition, mode power is also obtained from the mode excitation fraction and total power.

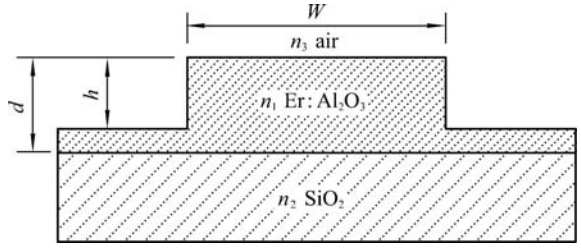

Fig. 1 Rib waveguide ($n_1 = 1.64$, $n_2 = 1.51$, $n_3 = 1$, $d = 1$ μm, $W = 3$ μm, $h = 0.8$ μm)

2.2 Rate equations

Figure 2 shows the energy level structure and the transition schematic of a Yb^{3+}-Er^{3+} co-doped system pumped at 0.98 μm. Considering the cooperative upconversion, excited state absorption, cross-relaxation and Yb-Er energy transfer, rate equations and conservation laws are founded as follows:

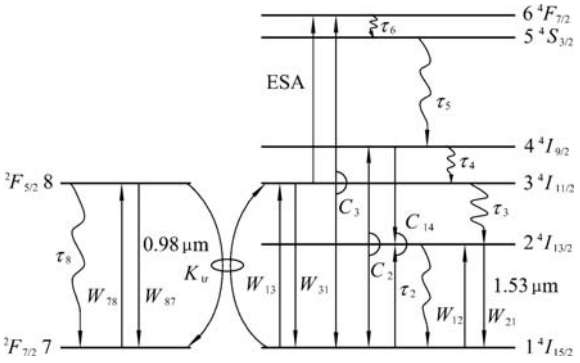

Fig. 2 Schematic representation of energy level and transition for Er^{3+}-Yb^{3+} co-doped system pumped at 0.98 μm.

$$\frac{dN_1}{dt} = -W_{13}N_1 - W_{12}N_1 + W_{21}N_2 + W_{31}N_3 + \frac{N_2}{\tau_2} + C_2N_2^2 + C_3N_3^2 - C_{14}N_1N_4 - K_{tr18}N_1N_8 + K_{tr37}N_3N_7, \quad (1)$$

$$\frac{dN_2}{dt} = W_{12}N_1 - W_{21}N_2 - \frac{N_2}{\tau_2} + \frac{N_3}{\tau_3} - 2C_2N_2^2 + 2C_{14}N_1N_4, \quad (2)$$

$$\frac{dN_3}{dt} = W_{13}N_1 - W_{31}N_3 - \frac{N_3}{\tau_3} + \frac{N_4}{\tau_4} - 2C_3N_3^2 - W_{ESA}N_3 + K_{tr18}N_1N_8 - K_{tr37}N_3N_7, \quad (3)$$

$$\frac{dN_4}{dt} = -\frac{N_4}{\tau_4} + \frac{N_5}{\tau_5} + C_2N_2^2 - C_{14}N_1N_4, \quad (4)$$

$$\frac{dN_5}{dt} = -\frac{N_5}{\tau_5} + \frac{N_6}{\tau_6}, \quad (5)$$

$$\frac{dN_6}{dt} = -\frac{N_6}{\tau_6} + C_3N_3^2 + W_{ESA}N_3, \quad (6)$$

$$\frac{dN_7}{dt} = -W_{78}N_7 + W_{87}N_8 + \frac{N_8}{\tau_8} + K_{tr18}N_1N_8 - K_{tr37}N_3N_7, \quad (7)$$

$$\frac{dN_8}{dt} = -\frac{dN_7}{dt}, \quad (8)$$

$$N_{Er} = N_1 + N_2 + N_3 + N_4 + N_5 + N_6, \quad (9)$$

$$N_{Yb} = N_7 + N_8, \quad (10)$$

where N_{Er} and N_{Yb} are the doping concentrations of Er and Yb, respectively, N_i and τ_i are the ion density and average lifetime of the ith level, respectively, C_2 and C_3 are the upconversion coefficients of the $^4I_{13/2}$ and $^4I_{11/2}$ levels, accordingly, and C_{14} is the cross-relaxation coefficient between $^4I_{15/2}$ and $^4I_{9/2}$. W_{12}, W_{21} and W_{13}, W_{31} are the stimulated absorption and stimulated emission transition probability for the signal and pump light, W_{ESA} is the excited state absorption transition probability ($^4I_{11/2} \rightarrow {}^4F_{7/2}$). K_{tr18} is the energy transfer coefficient from Yb^{3+} ($^2F_{5/2}$) to Er^{3+} ($^4I_{15/2}$). K_{tr37} is the reverse energy transfer coefficient from Er^{3+}($^4I_{11/2}$) to Yb^{3+}($^2F_{7/2}$), but this reverse energy transfer can be neglected due to the lifetime of a μs and few particles existing in level $^4I_{11/2}$.

Amplified spontaneous emission should be considered to exactly analyze the gain of an Er or Yb-Er co-doped amplifier. Three kinds of light exist in a waveguide: signal light, pump light and spontaneous emission (forward and backward), so

$$W_{12(21)}(x,y,z) = \frac{\sigma_{Er\text{-}a12(Er\text{-}e21)}(\nu_s)}{h\nu_s} I_s(x,y,z) + \sum_{j=1}^{M} \frac{\sigma_{Er\text{-}a12(Er\text{-}e21)}(\nu_j)}{h\nu_j} \times \left[I_{ASE+}(x,y,z,\nu_j) + I_{ASE-}(x,y,z,\nu_j)\right], \quad (11)$$

$$W_{13}(x,y,z) = \frac{\sigma_{Er\text{-}a13}(\nu_p)}{h\nu_p} I_p(x,y,z), \quad (12)$$

$$W_{ESA}(x,y,z) = \frac{\sigma_{ESA}(\nu_p)}{h\nu_p} I_p(x,y,z), \quad (13)$$

$$W_{78(87)}(x,y,z) = \frac{\sigma_{Yb\text{-}a78(Yb\text{-}e87)}(\nu_p)}{h\nu_p} I_p(x,y,z), \quad (14)$$

where $\sigma_{Er\text{-}a12}(\nu_s)$ and $\sigma_{Er\text{-}e21}(\nu_s)$ are the absorption and emission cross-sections of Er^{3+} at 1.53 μm, respectively. $\sigma_{Er\text{-}a13}(\nu_p)$ is the absorption cross-section of Er^{3+} at 0.98 μm, $\sigma_{Yb\text{-}a78}(\nu_p)$ and $\sigma_{Yb\text{-}e87}(\nu_p)$ are the absorption and emission cross-sections of Yb^{3+} at 0.98 μm, respectively. σ_{ESA} is the Er^{3+} excited-state absorption cross-section. I is the light intensity, M is the sampling number of frequency slots of width $\Delta\nu$ for a divided spontaneous emission spectrum (1.45–1.65 μm), and ν_j is the center frequency of each slot. $\sigma_{Er\text{-}a12}(\nu_j)$ and $\sigma_{Er\text{-}e21}(\nu_j)$ are the absorption and emission cross-sections for ν_j in the 1.45–1.65 μm band, respectively [6], which can be used to analyze the noise of the amplifier as well. The intensity distribution is expressed by normalized intensity distribution and actual power in a waveguide:

$$I_{s(p)}(x,y,z) = \psi_{s(p)}(x,y)P_{s(p)}(z), \quad (15)$$

$$I_{ASE\pm}(x,y,z,\nu_j) = \psi_s(x,y)P_{ASE\pm}(z,\nu_j). \quad (16)$$

$P_s(z)$, $P_p(z)$ and $P_{ASE\pm}(z, \nu_j)$ represent the power of the signal, pump and spontaneous emissions going forward and backward, respectively.

Analyzing the gain of the Er-doped waveguide amplifier, we set N_{Yb} as 0 cm^{-3} and the energy transfer coefficient between Yb and Er as 0. The optical parameters used in theoretical analysis are from the experimental data in related literature with Al_2O_3 as host material, which can be seen in Table 1 [1,8,9].

2.3 Propagation equations

The steady-state variation of the signal, pump and amplified spontaneous emission powers along the active waveguide are described by propagation equations [15]:

$$\frac{dP_p(z)}{dz} = -\gamma_p(z)P_p(z) - \alpha_p P_p(z), \quad (17)$$

$$\frac{dP_s(z)}{dz} = [\gamma_{21}(z,\nu_s) - \gamma_{12}(z,\nu_s)]P_s(z) - \alpha_s P_s(z), \quad (18)$$

$$\frac{dP_{ASE\pm}(z,\nu_j)}{dz} = \pm\left[\gamma_{21}(z,\nu_j) - \gamma_{12}(z,\nu_j)\right]P_{ASE\pm}(z,\nu_j) \pm mh\nu_j\Delta\nu\gamma_{21}(z,\nu_j) \mp \alpha_s P_{ASE\pm}(z,\nu_j), \quad j = 1,2,\ldots,M. \quad (19)$$

Here

$$\gamma_{12(21)}(z,\nu_s) = \iint_A \psi_s(x,y)\sigma_{Er\text{-}a12(Er\text{-}e21)}(\nu_s)N_{1(2)}(x,y,z)dxdy, \quad (20)$$

Table 1 Parameters of Yb^{3+}-Er^{3+} co-doped Al_2O_3 film

parameter		value					
pump cross-section ($\lambda_p = 0.98$ μm)	absorption	$\sigma_{Er\text{-}a13} = 1.7 \times 10^{-21}$ cm^2			$\sigma_{Yb\text{-}a78} = 11.7 \times 10^{-21}$ cm^2		
	emission	$\sigma_{Er\text{-}e31} = 0$ cm^2			$\sigma_{Yb\text{-}e87} = 11.6 \times 10^{-21}$ cm^2		
signal cross-section ($\lambda_s = 1.53$ μm)	absorption	$\sigma_{Er\text{-}a12} = 5.7 \times 10^{-21}$ cm^2					
	emission	$\sigma_{Er\text{-}e21} = 5.7 \times 10^{-21}$ cm^2					
excited state absorption cross-section		$\sigma_{ESA} = 0.8 \times 10^{-21}$ cm^2					
excited state lifetime		$\tau_2 = 7.8$ ms	$\tau_3 = 30$ μs	$\tau_4 = 1.0$ ns	$\tau_5 = 7.0$ μs	$\tau_6 = 20$ ns	$\tau_8 = 1.1$ ms
upconversion coefficient	$N_{Er} = 2.7 \times 10^{20}$ cm^{-3}	$C_2 = C_3 = C_{14} = 4.1 \times 10^{-18}$ cm^3/s					
(assuming a linearly increasing function of Er concentration)	$N_{Er} = 4.4 \times 10^{19}$ cm^{-3}	$C_2 = C_3 = C_{14} = 3.5 \times 10^{-18}$ cm^3/s					
energy transfer coefficient		$K_{tr18} = 4.0 \times 10^{-17}$ cm^3/s					

$$\gamma_{12(21)}(z,v_j) = \iint_A \psi_s(x,y)\sigma_{Er\text{-}a12(Er\text{-}e21)}(v_j)N_{1(2)}(x,y,z)\mathrm{d}x\mathrm{d}y, \tag{21}$$

$$\begin{aligned}\gamma_p(z) = \iint_A \psi_p(x,y)\big[&\sigma_{Er\text{-}a13}(v_p)N_1(x,y,z) \\ &+ \sigma_{ESA}(v_p)N_3(x,y,z) + \sigma_{Yb\text{-}a78}(v_p)N_7(x,y,z) \\ &- \sigma_{Yb\text{-}e87}(v_p)N_8(x,y,z)\big]\mathrm{d}x\mathrm{d}y.\end{aligned} \tag{22}$$

α_s and α_p are waveguide losses for the signal and pump, A is the cross-section area of the active region, and m is the number of guiding modes at signal wavelength, which is decided by the waveguide film dielectric constant and the geometric structure. For example, for double fundamental modes, $m = 2$.

The boundary condition for waveguide amplifiers is

$$P_p(0) = P_p, \quad P_s(0) = P_s, \quad P_{ASE+}(0,v_j) = P_{ASE-}(L,v_j) = 0,$$

where L is the waveguide length. The gain is given by

$$G = 10\lg\frac{P_s(z)}{P_s(0)}. \tag{23}$$

By FEM, the normalized intensity distributions ψ_s, ψ_p of the signal and pump are computed. The particle number $N_i(x, y, z)$ of each level could be achieved by solving the rate equations under steady-state, then $\gamma_p(z)$, $\gamma_{12}(z,v_j)$ and $\gamma_{21}(z,v_j)$ are calculated with ψ_s, ψ_p and N_i. Finally, $2M+2$ nonlinear differential equations, i.e., propagation equations, are solved by Runge-Kutta and a multi-step method. $P_{ASE\pm}(z,v_j)$, $P_s(z)$ and $P_p(z)$ are calculated step by step. The waveguide loss of the signal, spontaneous emission and pump light adopts a reference value of 0.35 dB/cm [8], and the step length is 20 μm.

By comparing the results of sampling number $M = 50$ ($\Delta\lambda = 4$ nm, $\Delta v = 512$ GHz) with $M = 200$ ($\Delta\lambda = 1$ nm, $\Delta v = 128$ GHz), the relative gain difference $(G_{200} - G_{50})/G_{200}$ varies from 1×10^{-6} to 1×10^{-3} at $N_{Er} = 2 \times 10^{20}$ cm^{-3}, $P_p = 50$ mW, $L = 15$ cm, so it is enough to divide the spontaneous emission spectrum into 50 frequency slots.

3 Gain characteristics of waveguide amplifiers

3.1 Comparison of pump efficiency and gain between EDAWA and YEDAWA

For EDAWA and YEDAWA, the typical result of pump efficiency and gain of the amplifier as pump power changes is shown in Fig. 3. The input signal power is $P_s(0) = 1$ μW (−30 dBm), Er concentration $N_{Er} = 2 \times 10^{20}$ cm^{-3}, Yb concentration $N_{Yb} = 5 \times 10^{20}$ cm^{-3}, and the waveguide length is 2 cm. It is clear from Fig. 3 that the higher the pump power is, the higher the gain is, and finally the gain tends toward saturation. The gain of YEDAWA reaches saturation at the pump power of 5 mW while EDAWA needs a higher pump power to reach saturation. In addition, the gain of YEDAWA is higher than that of EDAWA.

As for pump efficiency, YEDAWA is obviously higher than that of EDAWA, especially at low pump power. The pump efficiency will drop as pump power increases, so co-doping with Yb can not improve an amplifier's pump efficiency at high pump power.

3.2 Parameter optimization of amplifiers

Figure 4 illustrates that the net gains of EDAWA and YEDAWA vary with the amplifier length at different pump powers. As shown by the curves in Fig. 4, the gain increases at the beginning and then drops. In the initial stage, the signal light is so weak that the gain coefficient $\gamma_{21}(z,v_s) - \gamma_{12}(z,v_s)$ in Eq. (18) can be considered as constant, and the gain increases linearly along the waveguide. And then the gain increases slowly, which can be explained by two reasons. On one hand, as the signal light is amplified, the saturation effect leads to a low gain coefficient. On the other hand, as pump power is wasted in the amplification process, the pump efficiency drops and the population inversion decreases, which also reduces the gain coefficient and the gain increases slightly. When it reaches a certain length where the gain coefficient

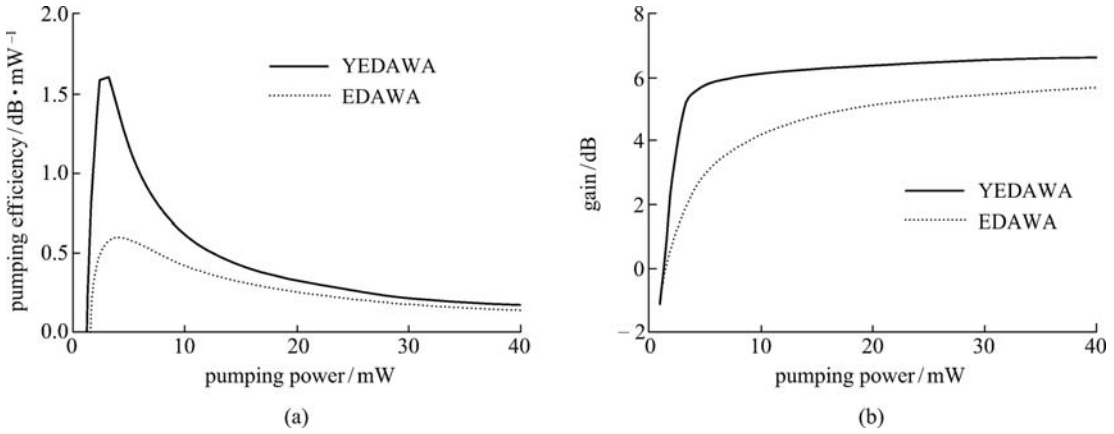

Fig. 3 Characteristic comparisons between YEDAWA and EDAWA. (a) Pumping efficiency comparison; (b) gain comparison

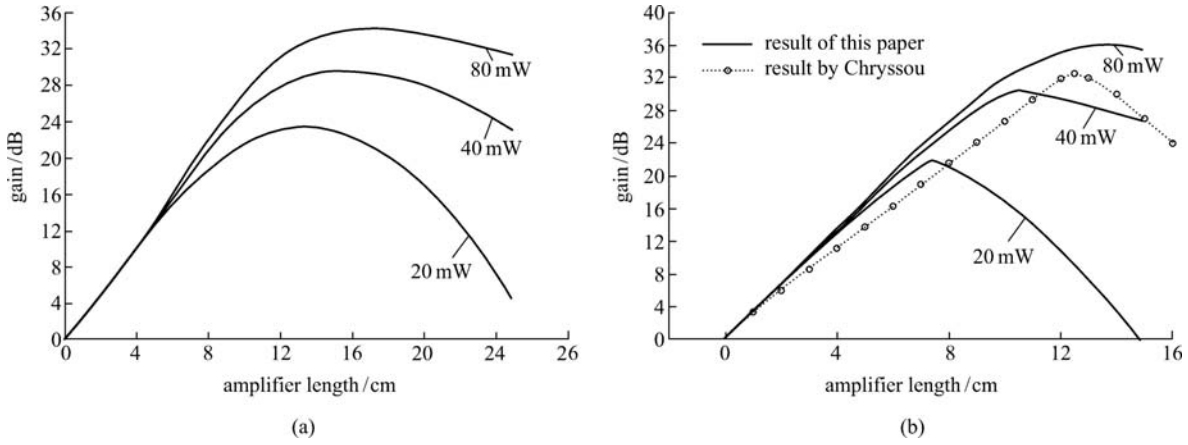

Fig. 4 Signal gain versus amplifier length for different input pump powers ($N_{Er} = 2 \times 10^{20}$ cm^{-3}, $N_{Yb} = 1 \times 10^{21}$ cm^{-3}). (a) EDAWA; (b) YEDAWA

equals the loss coefficient of the waveguide, the signal stops being amplified and the net gain comes to its maximum. If the length continues to increase, as the population inversion and the gain coefficient continue decreasing, even the loss and absorption surpass the gain, the signal light weakens, and the net gain begins to decrease. So there is an optimal waveguide length for the net gain of the amplifier which is relative to the pump power.

A linear characteristic is more obvious for YEDAWA in the region of increase and decrease of gain. A much longer waveguide and higher pump power are needed for higher gain. Under the conditions of Er concentration of 2×10^{20} cm^{-3} and pump power of 40 mW, the maximum gain for EDAWA is approximately 28 dB when the waveguide length is 16 cm, while approximately 32 dB can be achieved for YEDAWA with a waveguide length of only 10 cm under the same conditions.

Hoven et al. [8] theoretically predicted that the gain of a waveguide amplifier would achieve 20 dB for a 50 mW pump power at 1.48 μm, $N_{Er} = 2.7 \times 10^{20}$ cm^{-3} and 15 cm waveguide length. In this paper, using an optimized pump wavelength of 0.98 μm, an Er concentration of 2.0×10^{20} cm^{-3} and a waveguide length of 15 cm, we obtain a gain of 30 dB for 40 mW pump power.

Figure 4(b) also shows the theoretical results obtained by Chryssou [10], in which Er and Yb concentrations are identical and the pump power is 100 mW. However, Chryssou adopted a 2 μm × 2 μm channel waveguide so that the active region area is bigger and much higher pump power is needed. Furthermore, the signal propagates by way of multi-modes with E_{11}^x, E_{11}^y, E_{21}^x, E_{21}^y, E_{12}^x and E_{12}^y, and the amplification of the signal will bring mode dispersion, which is a disadvantage for the amplifier. So the pump efficiency of the rib waveguide amplifier introduced here is much higher than that of Chryssou. In addition, it can guarantee single mode propagation at signal wavelength.

Unlike the fiber amplifier, once a waveguide amplifier is fabricated, the length changes no more. For a certain pump power, the optimal length of the amplifier is such that the remaining pump power would make the net gain

coefficient just equal to zero at the end of the amplifier; here the net gain reaches the maximum. The doping concentration indeed affects the optimal length as well. We conclude that an optimum matching relation exists among optimal length, doping concentration and pump power. For EDAWA, optimizing the three parameters synchronously, we get a practical optimization design curve as shown in Fig. 5. The horizontal axis denotes the pump power and the vertical axis denotes the optimized waveguide length; dashed lines mean Er concentration lines and the solid lines show contour lines of the maximum gain. The intersection point of the four parameters means that the corresponding maximum gain could be obtained under the condition of the corresponding pump power, Er concentration and optimal length. We can also choose suitable parameter values based on the experimental condition at hand to win the appropriate gain.

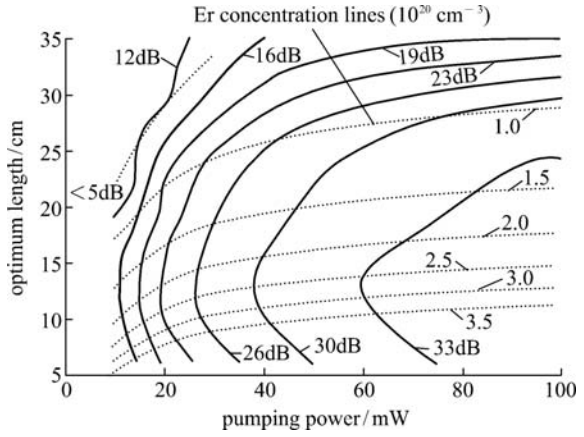

Fig. 5 Multi-parameter optimum of Er-doped Al_2O_3/SiO_2 waveguide amplifier

4 Experimental research of YEDAWA based on SiO_2/Si

Yb-Er co-doped Al_2O_3 thin film [16–19] based on SiO_2/Si is fabricated by medium frequency sputtering. The process includes: thermally oxidizing the Si (100) substrate; ultrasonic cleaning; depositing the Yb-Er co-doped Al_2O_3 film onto the surface of SiO_2 by twin targets medium frequency magnetron sputtering technology in a vacuum chamber; and, annealing the films at 850°C. The sputtering twin targets are two identical aluminum targets wherein a certain number of Er and Yb cylinders of Φ2 mm are embedded in the desired proportion. The twin targets are alternatively used as cathode and anode, which cannot only inhibit the arc discharge on the sputtering targets surfaces, but also eliminate "anode disappearing" in the usual DC magnetron sputtering and the instability of plasma discharge.

The Al_2O_3 film obtained is compact and homogeneous, with a layer thickness of 1.16 μm, refractive index of 1.65, Er concentration of 0.6 at.%, Yb concentration of 5.2 at.% and a size of 22.4 mm × 10.6 mm. The photoluminescence (PL) spectrum peak is around 1.53 μm, and FWHM is 40–60 nm. The film was etched by the Chuangweina Company in Beijing. Because of the difficulty in Al_2O_3 etching, the sample waveguide made at present is a nonstandard rib waveguide which is 10 μm wide, 1.04 μm high, 2.24 cm long; the waveguide space is 30 μm and there is air cladding.

The characteristics of the fabricated waveguide amplifier are theoretically simulated by the multi theory model. The finite element analysis shows that the multi modes propagate at both signal and pump wavelengths. Signal wavelength has six *x*-polarized modes and the pump wavelength has twenty-six modes. Because the big cross-section of the waveguide decreases the pump power density, the threshold pump power is bigger.

Pump and signal beams are combined into a single mode fiber using a wavelength division multiplexer. The end of the fiber was tapered from 8.2 μm to Φ0.96 μm. Pump and signal are directly coupled into the waveguide by means of a five-dimensional fiber regulator with precision in nanometers. Through an optical chopper (425 Hz) and a band-pass filter with a central wavelength of 1.54 μm and a bandwidth of 26 nm, the amplified signal received by an InGaAs detector, amplified by lock-in, is displayed and the data are processed by computer. In our experiment, the power supply of the signal is modulated at 1 Hz, and then the peak-to-peak value is measured. This not only separates the pump completely but also eliminates the amplified spontaneous emission and random scattered light. The measurement is done at room temperature.

Figure 6 gives the results of the experiment, showing that the amplifier gain varies with the pump power. The threshold pump power is around 18 mW, and the net gain can reach 8.44 dB at 70 mW pump power, which equals a gain of 3.77 dB/cm. The figure also shows the simulation results using the multi-theoretical model. The

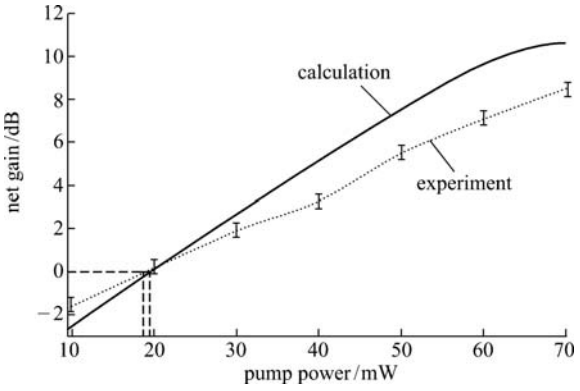

Fig. 6 Dependence of net gain of YEDAWA on pump power

experimental data are in accordance with the numerical simulation results, and the two threshold pump powers are also very close.

The 2.24 cm YEDAWA gets a net gain of 10.6 dB (4.73 dB/cm) by theoretical calculation; the reason for the difference is that the optical parameters used here may be different from the actual parameters. Even though the host materials are identical, the preparation methods and techniques are different [20]. In addition, the waveguide loss in calculation is 0.35 dB/cm, whereas the actual waveguide loss is perhaps a little larger, such as the scattering loss caused by interface flatness of the waveguide. It can be improved by enhancing film fabrication and etching techniques.

5 Conclusion

The gain characteristics of EDAWA and YEDAWA are analyzed by the multi-theoretical model, including rate equations, finite element field distribution, and propagating equations with forward and backward spontaneous emission. In the simulation, a more reasonable optimized program of parameters is established, which can achieve the synchronous optimization of pump power, doping concentration, waveguide length and gain. The optimum design curve is charted. The theoretical model is applied to a practical Yb-Er co-doped Al_2O_3 waveguide amplifier, and the results show that the calculations are in good agreement with the experimental data.

References

1. van den Hoven G N, Snoeks E, Polman A, et al. Upconversion in Er-implanted Al_2O_3 waveguides. Journal of Applied Physics, 1996, 79(3): 1258–1266
2. Kozanecki A, Sealy B J, Homewoos K. Excitation of Er^{3+} emission in Er, Yb co-doped thin silica films. Journal of Alloys and Compounds, 2000, 300–301: 61–64
3. Polman A. Erbium-doped planar optical amplifiers. In: Proceeding of 10th European Conference on Integrated Optics (ECIO'01), 2001, 75–78
4. Zhang Long, Lin Fengying, Qi Changhong, et al. High erbium-doped glasses for waveguide amplifiers at 1.53 μm. Acta Optica Sinica, 2000, 20(12): 1688–1693 (in Chinese)
5. Cheng Haiyan, Dai Jizhi, Yang Yapei, et al. Er^{3+}, Yb^{3+} codoped phosphate glass channel waveguide amplifiers. Acta Optica Sinica, 2003, 23(7): 815–818 (in Chinese)
6. van den Hoven G N, Van der Elsken J A, Polman A, et al. Absorption and emission cross sections of Er^{3+} in Al_2O_3 waveguides. Applied Optics, 1997, 36(15): 3338–3341
7. Gapontsev V P, Matitsin S M, Isineev A A, et al. Erbium glass lasers and their applications. Optics & Laser Technology, 1982, 14(4): 189–196
8. van den Hoven G N, Koper R J I M, Polman A, et al. Net optical gain at 1.53 μm in Er-doped Al_2O_3 waveguides on silicon. Applied Physics Letters, 1996, 68(14): 1886–1888
9. Strohhofer C, Polman A. Absorption and emission spectroscopy in Er^{3+}-Yb^{3+} doped aluminum oxide waveguides. Optical Materials, 2003, 21(4): 705–712
10. Chryssou C E, Di Pasquale F, Pitt C W. Improved gain performance in Yb^{3+}-sensitized Er^{3+}-doped alumina (Al_2O_3) channel optical waveguide amplifiers. Journal of Lightwave Technology, 2001, 19(3): 345–349
11. Di Pasquale F, Zoboli M, Federighi M, et al. Finite-element modeling of silica waveguide amplifiers with high erbium concentration. IEEE Journal of Quantum Electronics, 1994, 30(5): 1277–1282
12. Lopez-Barbero A P, Hernandez-Figueroa H E, Torres P. Numerical modeling of multimode doped optical waveguides. Advances in Engineering Software, 2000, 31(4): 235–240
13. Li Shufeng, Song Changlie, Li Chengren, et al. Theoretical model of Er-doped Al_2O_3 waveguide amplifier. Proceedings of SPIE, 2002, 4927: 263–270
14. Li Shufeng, Song Changlie, Li Chengren, et al. Coupling of fiber-waveguide amplifier. Proceedings of SPIE, 2004, 5644: 250–258
15. Giles C R, Desurvire E. Modeling erbium-doped fiber amplifiers. Journal of Lightwave Technology, 1991, 9(2): 271–283
16. Gao Jingsheng, Song Changlie, Li Chengren, et al. Photoluminescence of Yb^{3+}/Er^{3+} co-doped Al_2O_3 film fabricated by medium frequency sputter. Journal of Optoelectronics·Laser, 2004, 15(10): 1162–1165 (in Chinese)
17. Li Chengren, Song Changlie, Li Shufeng, et al. Deposition of Er^{3+}:Al_2O_3 films by closed-field unbalanced magnetron sputtering and photoluminescence characterization of the films. Proceedings of SPIE, 2002, 4905: 617–622
18. Song Qi, Song Changlie, Gao Jingsheng, et al. Yb^{3+}/Er^{3+} co-doped Al_2O_3 optical waveguide fabricated by middle frequency sputter. Laser Technology, 2005, 29(4): 440–445 (in Chinese)
19. Li Chengren, Li Shufeng, Song Qi, et al. Characteristics of net gain of Yb:Er co-doped Al_2O_3 waveguide amplifier. Acta Photonica Sinica, 2006, 35(5): 650–654 (in Chinese)
20. Kik P G, Polman A. Cooperative upconversion as the gain-limiting factor in Er doped miniature Al_2O_3 optical waveguide amplifiers. Journal of Applied Physics, 2003, 93(9): 5008–5012